Low energy electron scattering in CF_2Cl_2 and CF_3Cl

D. Field[a] and N. C. Jones
Institute of Physics and Astronomy, University of Aarhus, DK-8000 Aarhus C, Denmark

S. L. Lunt[b]
Institute for Storage Ring Facilities, University of Aarhus, DK-8000 Aarhus C, Denmark

J.-P. Ziesel
Laboratoire Collisions Agrégats Réactivité, Université Paul Sabatier, 31062 Toulouse, France

R. J. Gulley
AMPL, RSPhysSE, Australian National University, ACT 0200, Australia

(Received 7 March 2001; accepted 4 June 2001)

Experimental data are presented for the scattering of electrons by CF_2Cl_2 and CF_3Cl for both integral and backward scattering, from 2 eV (for CF_2Cl_2) and 0.65 eV (for CF_3Cl) down to energies of 10 meV to 20 meV, with an energy resolution ranging from 0.75 meV to 1.5 meV (full width at half maximum) in the electron beam. Both molecules have dipole moments of ~0.5 D and are expected to show very similar rotationally inelastic scattering cross sections. Cross sections for CF_2Cl_2 are, however, much larger at low energy than for CF_3Cl, attributed to short-lived attachment of electrons to CF_2Cl_2. CF_3Cl displays powerful suppression of rotational excitation in the forward direction, most strongly around 70 meV impact energy. This is ascribed to interference between a direct channel of rotational excitation and indirect excitation via a short-lived negative ion state. [DOI: 10.1063/1.1387475]

I. INTRODUCTION

Electron scattering and dissociative attachment with chlorofluorocarbons (CFCs) has been intensively studied both experimentally and theoretically in recent years, e.g., Refs. 1–21. CF_2Cl_2 and CF_3Cl display a rich sequence of phenomena including shape resonant enhanced vibrational excitation,[3,4] electron attachment, e.g., Refs. 7, 9, 13, 22–24, and rotationally inelastic scattering.[5] CF_2Cl_2 and CF_3Cl were indeed the first species in which near-threshold rotationally inelastic electron scattering was observed. Absolute values for scattering cross sections for CF_2Cl_2 and CF_3Cl may be found in Refs. 7, 6, and 25.

In contrast to the numerous studies involving electron swarms or dissociative attachment, reviewed most recently in Refs. 9 and 21, all earlier work involving electron beam scattering has involved collision energies greater than ~300 meV. The exception is in Ref. 5, but this study reported only backward scattering data and did not record absolute scattering cross sections. In the present work we perform electron beam transmission spectroscopy reporting absolute cross sections for electron scattering down to energies of 10–20 meV for CF_2Cl_2 and CF_3Cl. Results are reported for both integral and backward scattering. These data provide new insight into the nature of rotationally inelastic scattering in polar molecules, revealing for example a remarkable suppression of rotational excitation below 100 meV for CF_3Cl and greatly enhanced cross sections for scattering by CF_2Cl_2. Data also provide further tests of the accuracy of the first order Born point-dipole approximation in estimating rotationally inelastic scattering cross sections in electron collisions with polar molecules. Tests of Born theory are important since, in the absence of experimental values, Born calculations remain the only source of data for rotationally inelastic cross sections. Values of cross sections are necessary to model RF plasmas used in microelectronic device fabrication, as we outline below. Earlier work has shown that Born calculations are not reliable and agreement between experimental and theoretical values is both variable and unpredictable below a few hundred meV electron impact energy.[26–32] Agreement between theory and experiment in the present case is poor in the case of CF_3Cl. A direct comparison cannot be made for CF_2Cl_2.

We expand briefly here on the relevance of rotationally inelastic scattering in RF discharges. The electron temperature is one of the defining parameters of these systems, determining, for example, the potential of the plasma relative to a floating object in the plasma, such as a wafer undergoing processing.[33,34] The ability of molecules to cool electrons to the kinetic temperature of a typical RF plasma is largely determined by the presence of polar species, since such species display very large rotationally inelastic cross sections in collisions with electrons.[26–32] Industrial RF processes typically use chlorinated and brominated gases, which tend to be strongly electron attaching in the presence of low energy electrons. Cool electrons formed through rotationally inelastic scattering may then be siphoned off by these electron attaching species in the plasma, depleting the system of electrons via negative ion formation. This fundamentally alters the electrical properties of the discharge.

[a]Author to whom correspondence should be addressed. Electronic mail: dfield@ifa.au.dk
[b]Present address: Therma VG Scientific, The Birches Industrial Estate, Imberhorne Lane, East Grinstead, West Sussex RH19 1UB, United Kingdom.

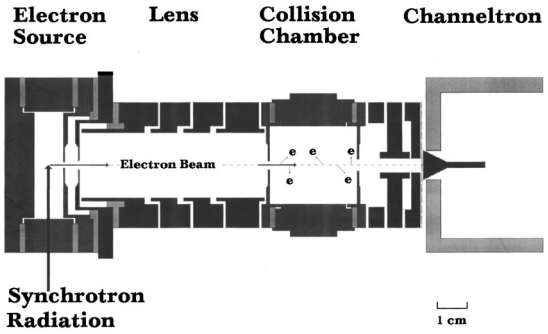

FIG. 1. A schematic diagram of the apparatus. Monochromatic synchrotron radiation enters the photoionization electron source containing argon, at low ambient pressure of typically a few tenths of 1 Pa. Photoelectrons, expelled by a weak electric field, are focused by a 4-element lens (Ref. 39) into a collision chamber containing the target gas. Transmitted electrons are detected at the channel electron multiplier (''channeltron'') situated beyond some further electron optics.

II. EXPERIMENTAL METHOD

The experiment uses a synchrotron photoionization source of electrons to provide scattering data at an energy resolution in the incident electron beam (see below) of between 0.75 meV and 3.5 meV, where beam energies in the present work range from ~10 meV to 2 eV. The apparatus has been described in detail previously[35,36] and is based upon that described in Ref. 37. In brief, electrons are formed by photoionization of Ar using monochromatized synchrotron radiation at the sharp autoionizing resonance Ar** $3p^5(^2P_{1/2})11s$ superposed on the broad $9d'$ resonance at 78.65 nm,[38] ~4 meV above the $^2P_{3/2}$ ionization threshold. The experimental system consists of a photoionization region, electrostatic optics to convey electrons to a collision cell containing the target gas and a channel electron multiplier for recording the electron current. The entire system may be immersed in an axial magnetic field of strength $\sim 2 \times 10^{-3}$ T.[35]

A schematic diagram of the apparatus is shown in Fig. 1. Synchrotron radiation is focused at the center of the region of photoionization into a strip typically less than 10 μm in thickness, representing a demagnified image of the exit slit of the monochromator. The photoelectrons are formed into a beam using a weak electrostatic draw-out field across the photoionization chamber. In the absence of the magnetic field, the draw-out field is typically 0.2 V/cm. In presence of the magnetic field, high draw-out efficiency may be achieved with lower electrostatic fields. In the present work draw-out fields of between a few tens of mV/cm and 120 mV/cm were used. The electron beam passes through a 1.8 mm aperture in the photoionization chamber and enters a system of electron optics, composed of a Calbick lens and a 4-element electrostatic zoom lens.[39] This serves to focus the electron beam into a field-free collision chamber of length 30 mm in which the room-temperature target gas is contained. The diameter of the entrance aperture of the collision chamber is 2.0 mm and of the exit aperture is 3.0 mm. Unscattered electrons are transported beyond the collision chamber via further optical elements and pass through a shielding mesh before detection at a channel electron multiplier (Galileo channeltron 7010M).

The electron energy is scanned by varying the potential in the photoionization source. Cross sections are measured through attenuation of the incident beam and evaluated using the Beer–Lambert Law,

$$I(t) = I(0)\exp(-\sigma n l), \tag{1}$$

where $I(0)$ and $I(t)$ are the unattenuated and attenuated electron currents, respectively, σ is the scattering cross section (see below), n is the target gas number density, and l is the effective path length of electrons through the target gas. The pressure in the target cell was measured either with a Leybold rotating ball gauge (Viscovac VM212) or a capacitive manometer (Edwards 655).

Spectra were obtained by scanning the electron energy with dwell times at any energy of 1–2 s with a step size of between 1 meV and 10 meV. Several spectra were summed to provide the data reported here. In order to obtain accurate values of scattering cross sections, experiments were also carried out at a variety of fixed electron impact energies. For each energy, a succession of five pairs of measurements was performed, integrating the attenuated and unattenuated currents over a period of 120 s in each case. Account was taken of the slow decrease in time of the incident electron beam associated with the declining current in the storage ring. The attenuation of the incident electron beam was maintained at 10%–20% or lower. A range of pressures was used to check that the derived cross sections were pressure independent and thus that multiple scattering did not make any appreciable contribution to the measurements.

In the absence of the magnetic field, the cross section obtained using Eq. (1) is the total integral cross section, σ_t, where ''total'' refers to all elastic and inelastic events and ''integral'' refers to integration over the full 4π steradians (but see below). In Eq. (1), the effective path length, l, of the electrons through the target gas has been experimentally determined through extensive experiments with N_2 and comparison with results in Refs. 40 and 41. These investigations show that within experimental error the geometrical length of the collision cell (30 mm) is an accurate measure of l. Further details may be found in Ref. 28.

In the present work, since the molecular targets possess sizable dipole moments, dipole scattering makes a strong contribution to the total scattering cross section at low collision energy. Dipole scattering has the well-known characteristic that electrons are strongly forward-scattered, e.g. Refs. 26–30. Thus a systematic underestimate of the total scattering cross section is unavoidable in transmission experiments, since a proportion of rotationally inelastically scattered electrons will pass through the exit aperture of the collision chamber and be detected as unscattered.[42] All integral cross sections reported here in the lower energy regime therefore suffer from this systematic error, the extent of which is discussed further in Sec. III.

In separate experiments in the presence of the axial magnetic field, any electrons scattered into the forward hemisphere by the target gas are realigned to perform forward-moving helical trajectories around the axis of the field and

are detected as unscattered. All electrons scattered into the backward hemisphere follow backward-moving trajectories around the direction of the magnetic field. These electrons are lost to the incident beam. The cross section measured is the total backward scattering cross section, σ_b, that is, the cross section for all events which cause electrons to be scattered into the backward 2π steradians. Above a certain energy, in the presence of the magnetic field, electrons scattered at close to 90° will have sufficient transverse energy to cause them to move in a spiral path with a diameter such that they cannot pass through the exit hole of the target gas cell. For electrons on axis, this energy is ~800 meV, but the energy is lower for off-axis incident electrons. In order to determine the energy to which absolute backward scattering cross-sections are reliable, backward cross sections have been measured in N_2 and compared with differential cross sections given in Ref. 41 integrated between 90° and 180°. Good agreement was found up to ~650 meV, which is therefore the limit of energy to which we quote backward scattering cross-sections.

The absolute electron energy scale is calibrated by observing the peak in the $N_2^-\ ^2\Pi_g$ resonance around 2.44 eV. Results in Refs. 43–45 indicate that the peak recorded in the total cross section at 2.440 eV is a good energy calibrator for both total and backward-scattering data, and thus for experiments with and without the magnetic field present. We assign an energy of 2.442 eV to this peak, this figure being the average of the values of 2.444 eV and 2.440 eV in Refs. 43 and 44, respectively. Discrepancies between the N_2 resonance energy and electron energies estimated from potentials in the system typically lay between 10 meV and 50 meV, and did not vary significantly over the course of many experiments. We estimate that the absolute energy scale in the present data is accurate to ±5 meV, and rather better at energies below a few tens of meV.

The experimental data reported here were obtained at both the ASTRID storage ring (Institute for Storage Ring Facilities, University of Aarhus), using the undulator beamline equipped with a spherical grating monochromator, and the Synchrotron Radiation Source (SRS) at Daresbury Laboratory, using the VUV3.2 bending magnet beamline equipped with a 5 m McPherson normal incidence monochromator. Experimental data are shown in Figs. 2 and 3 for CF_2Cl_2 and in Fig. 4 for CF_3Cl. Total integral cross sections for CF_2Cl_2 were obtained at ASTRID, with a photon resolution of 1.5 meV full width at half maximum (FWHM). The backward scattering data in Fig. 3 were obtained at the SRS with a photon resolution of ~3.5 meV FWHM. These data also include a number of additional cross section determinations using ASTRID (resolution 1.5 meV) in order to verify consistency of pressure measurements. Total integral cross sections for CF_3Cl, the upper set of points in Fig. 4, were obtained at ASTRID, with a photon resolution of 1.5 meV (FWHM). The backward scattering data in Fig. 4 in the energy range 20–50 meV were obtained at ASTRID, with a photon resolution of 0.75 meV FWHM, and between 50 and 650 meV at the SRS with a photon resolution of ~3.5 meV FWHM.

The values of photon resolution quoted above were determined from the observed form of threshold photoionization resonances in the spectrum of Ar. The energy distribution of the electrons is given by a convolution of the photon bandwidth of the ionizing radiation and the form of the combined 11s resonance, of width 0.09 meV,[46] and the $9d'$ resonance, of width ~6 meV. For the purposes of the present work the energy resolution of the photoelectrons may be taken to be that of the photon bandwidth quoted above. This behavior was demonstrated in Ref. 47 for data taken using the SRS. We presently have no independent observations of very sharp electron scattering features to confirm the higher resolution associated with the spherical grating monochromator on the ASTRID synchrotron.

Doppler motions of the room temperature target gas degrade the effective experimental resolution in the present experiments by less than 0.5% for collisions at 10 meV impact energy, rising to a few % at 100 meV.[48]

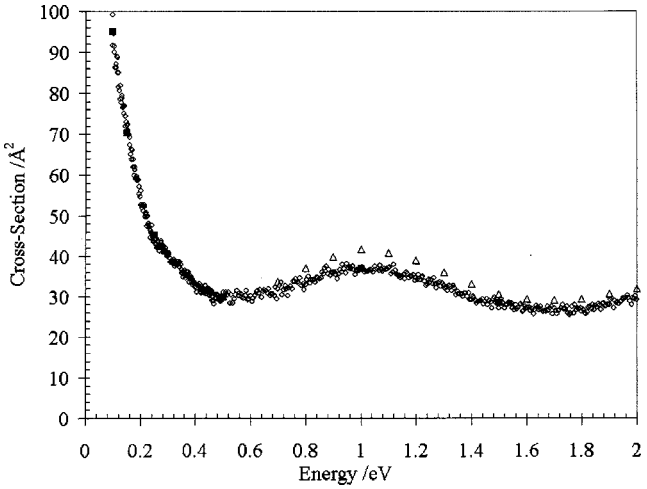

FIG. 2. CF_2Cl_2: total integral electron scattering cross sections vs electron energy in the energy range from 0.1 to 2 eV. Data of Ref. 25 (open triangles) are shown for comparison. Solid squares represent values taken at fixed electron energies (see Sec. II).

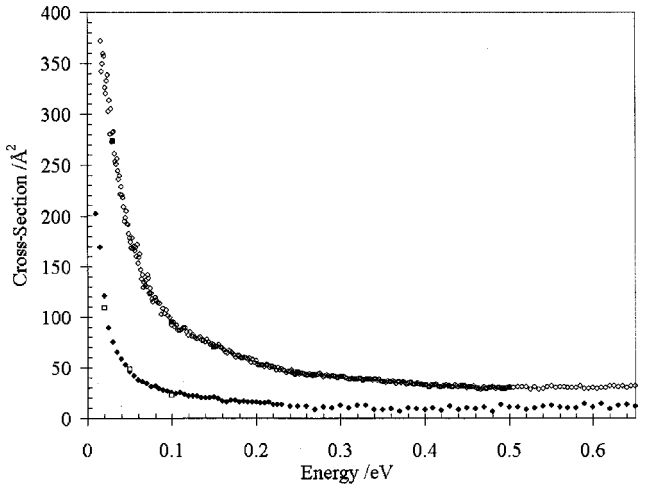

FIG. 3. CF_2Cl_2: total integral electron scattering cross sections (upper set) and total backward scattering cross sections (lower set) vs electron energy in the energy range up to 0.65 eV. Solid squares in the upper set of data and open squares in the lower set represent values taken at fixed electron energies.

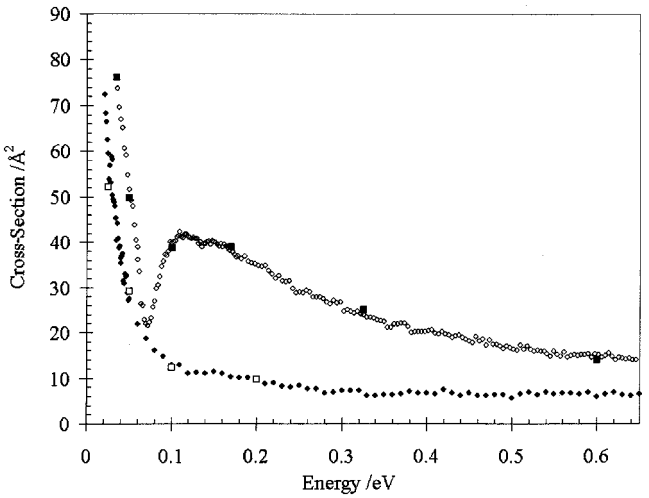

FIG. 4. CF_3Cl: total integral electron scattering cross sections (upper set) and total backward scattering cross sections (lower set) vs electron energy in the energy range up to 0.65 eV. Solid squares in the upper set of data and open squares in the lower set represent values taken at fixed electron energies.

Uncertainties in the reported cross sections arise from a number of sources including pressure measurements, random fluctuations in the electron beam intensities, and uncertainties in calibration of the path length of the electrons through the collision cell. These uncertainties correspond to an error of $\pm 5\%$ (one standard deviation) in the quoted cross sections.

III. DISCUSSION OF RESULTS

A. CF_2Cl_2

For both CF_2Cl_2 and CF_3Cl, the processes which may contribute to the measured cross sections are elastic scattering, rotationally inelastic scattering, vibrationally inelastic scattering, and attachment with or without molecular dissociation. Since the dipole moments of CF_2Cl_2 and CF_3Cl are essentially equal, it is quite remarkable that the total scattering cross section at 20 meV, for example, is greater by a factor of ~ 5 for integral scattering in CF_2Cl_2 compared with CF_3Cl (see Figs. 3 and 4).

Figure 2 shows that our present data lie systematically $\leqslant 10\%$ lower than those of Ref. 25 in the resonance region around 1 eV, possibly due to our poorer ability than Ref. 25 to detect forward scattering associated with vibrationally inelastic collisions in this energy region.[4] Small angle scattering is detected down to angles around 6° in the present experiment (see Sec. IV), whereas this figure is 0.3° in Ref. 25, as detailed in Ref. 49. At lower energies, data in Ref. 5, involving backward scattering cross sections, showed a weak feature associated with threshold vibrational excitation between 120 and 170 meV, which cannot be discerned above the noise in the present data. This arises because in Ref. 5 there was no accurate measurement of target pressure and in retrospect we realize that a very high pressure was used which artificially accentuated this feature. This same comment applies to data for CF_3Cl.[50]

Data for CF_2Cl_2 in Fig. 2 show that cross sections pass through a shallow minimum around 500–600 meV, attributed by Ref. 4 to a Ramsauer–Townsend effect. The weakness of the Ramsauer–Townsend effect might be due to the fact that only a rather small proportion of the total scattering cross section is due to s-waves. As Ref. 4 notes, rotationally inelastic scattering is in evidence at the energy of the minimum in the cross section and this involves many higher partial waves. However these data may equally be interpreted in terms of a drop in vibrationally inelastic scattering with rotationally inelastic scattering, or other processes (see below), taking over at lower energy. The importance of the presence or absence of a Ramsauer–Townsend effect in CF_2Cl_2 will become clear below.

We now compare our experimental results for the lower energies with the predictions of the first-order Born point dipole approximation for rotational excitation. The theory of rotational excitation of molecules by slow electrons has been reviewed by Refs. 51 and 52, and references therein. Expressions are derived in Ref. 53 for the scattering of electrons from polar symmetric top molecules. For simplicity we adopt the formalism of a symmetric top for CF_2Cl_2, noting that the determining factor in the magnitude of rotationally inelastic scattering cross sections is the dipole moment of the target, rather than details of the level structure or of the specific transitions involved. The asymmetry parameter $\kappa(=(2B-A-C)/(A-C))$ is -0.6 (Ref. 54) and CF_2Cl_2 is therefore quite close to a prolate symmetric top. We recognize that the approximation of CF_2Cl_2 to a symmetric top has the consequence that account may not be taken of the correct nuclear spin statistics in calculating rotational populations. However in a full description these effects would be small, since weights are in the ratio 9:7.[55] In addition we are bound in our simulations to the symmetric top selection rule $\Delta K = 0$, although CF_2Cl_2 undergoes μ_b transitions with the accompanying selection rule $\Delta K = \pm 1$. In Ref. 5, we adopted the rather different approach of using the formalism for scattering for a symmetric top, but adapting the relevant $3j$-symbol [in Eq. (2) below] to allow $\Delta K = \pm 1$ transitions. Results differ by a few percent from those reported here.

Basing our analysis on that of Crawford (1967), a pure rotational scattering cross section in SI units between the rotational levels (J,K) and (J',K), integrated between the two angles θ_1 and θ_2, may be expressed as

$$\sigma(J,K;J',K') = \xi(2J+1)\begin{pmatrix} J & J' & 1 \\ K & -K & 0 \end{pmatrix}^2 \times \ln\left[\left|\frac{(k^2+k'^2-2kk'\cos\theta_2)}{(k^2+k'^2-2kk'\cos\theta_1)}\right|\right], \quad (2)$$

where $\xi = (4\pi/3k^2)(\mu^2/(ea_0)^2)$.

In Eq. (2), J is the total angular momentum quantum number of the free molecule and K its effective projection on the molecular axis, in symmetric top terms. k' and k are the magnitudes of the final and initial wave vectors given by $k = (2m_eE)^{1/2}/\hbar$, where m_e and E are the mass and energy of the electron, $ea_0 = 8.4784\times 10^{-30}$ C m and μ is the dipole moment of the target molecule expressed in C m. For CF_2Cl_2, $\mu = 0.51$ D, where 1 D $= 3.335\,64\times 10^{-30}$ C m. The Wigner $3-j$ symbols in Eq. (2) are evaluated using the tables given in Ref. 56.

In order to simulate the rotationally inelastic contribution to the experimental scattering spectra for CF_2Cl_2, the Boltzmann populations of the target molecular rovibrational levels must be calculated. We consider target populations up to a maximum value of $J=100$ and populations of vibrational levels up to $\sim 700\ cm^{-1}$ involving $\nu_{3,4,5,7,9}$ including double excitation of ν_4 and ν_5.[4] Vibrationally inelastic scattering at threshold is not however included, since our spectra indicate that it is too weak to be detected within our signal to noise. The energies of rotational levels were calculated using rotational constants given in Ref. 54. As indicated above, we use selection rules appropriate for a prolate symmetric top implicit in Eq. (2), namely, $\Delta J=0,\pm 1$ and $\Delta K=0$. Spectra are simulated by combining at any energy all contributions from rotationally inelastic events, folding in a gaussian energy distribution for the incident electrons, in this case of 1.5 meV for total integral scattering data and 3.5 meV FWHM for backward scattering data.

The geometry of the collision chamber dictates that we omit to record a part of the cross section associated with low angle scattering, as noted in Sec. III. The problem of the nondetection of forward scattering has been dealt with at some length in Ref. 42. We follow the method used in that paper in order to calculate the effective rotationally inelastic Born cross section for integral scattering. Thus, in order to compare the predictions of the Born theory with experimental results, theoretical values are estimated from Eq. (2) using a range of values of θ_1, appropriate to the cell-length of 30 mm and exit hole diameter of 3 mm. We use a coarse numerical integration over the distance along the collision chamber, for each distance using an appropriate value of angle θ_1, with $\theta_2=180°$, referring to Eq. (2). This corrected cross section may be expressed as $l^{-1}\int_0^l dl[\sigma_{\mathrm{Born}}]_{\theta_1}^{2\pi}$, where σ_{Born} is the cross section calculated from Born theory for on-axis electrons for the appropriate value of l (which dictates the value of θ_1). We have used 9 values of θ_1 between 3° and 27°, corresponding to a set of equidistant points along the collision chamber. All theoretical results reported in the present work refer to calculations of the Born scattering cross section involving this effective reduction in the full angular range.

The above correction procedure predicts that ~30% of the integral cross section is unrecorded at 10 to 20 meV electron impact energy and approaching 50% at several hundred meV energy, given the geometry of our experiment. However experimental data for rotationally inelastic scattering show in every case that the Born theory strongly underestimates the relative contribution of low energy backward scattering in polar molecules.[26–32] The systematic errors quoted are therefore upper limits and the fraction of the integral scattering cross-section unrecorded for rotationally inelastic scattering is very considerably less than 30%.

A comparison between the predictions of Born theory and experimental cross sections is shown in Fig. 5. In this and subsequent similar comparisons, we ignore contributions from elastic scattering. This is a very good approximation in the energy regime below 100–200 meV where rotationally inelastic scattering strongly dominates. At higher energies pure elastic scattering will form an increasing proportion of the total cross-section. For example, data in Ref. 4 suggest that elastic scattering contributes ~15 $Å^2$ at 0.5 eV, noting however that these so-called elastic data include rotational excitation. At all events, the Born values in Fig. 5 are almost an order of magnitude too low for backward scattering and more than a factor of 2 too low for integral scattering below 100 meV impact energy. In addition the ratio of backward to integral scattering predicted by Born remains roughly constant in the low energy region and equal to ~0.1. The experimental value of the ratio is ~0.275, at 100 meV collision energy, rising to 0.45 at the lowest energy. This is shown in Fig. 6. These discrepancies in absolute values and in ratios between the prediction of the Born theory and observations are in excess of those generally encountered.[26–31] If we also consider that scattering cross sections are very much greater for CF_2Cl_2 than for CF_3Cl, we conclude that an additional mechanism other than rotational scattering operates in the scattering of electrons by CF_2Cl_2.

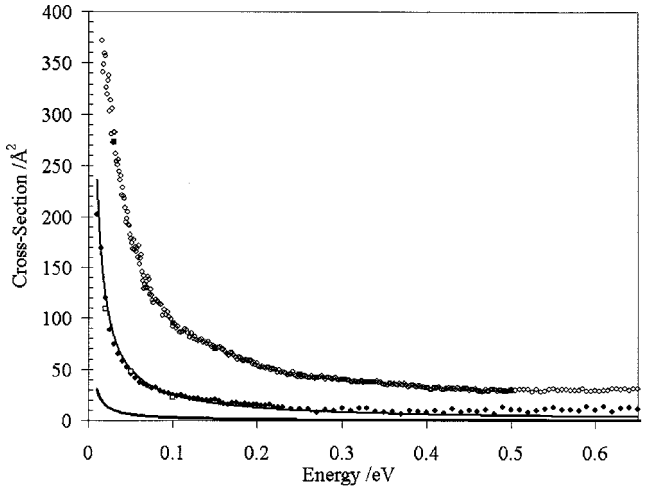

FIG. 5. CF_2Cl_2: experimental electron scattering cross sections vs electron energy as in Fig. 3 shown with cross sections calculated using the first order Born point-dipole approximation. Upper solid line: calculated integral cross sections. Lower solid line: backward scattering cross sections.

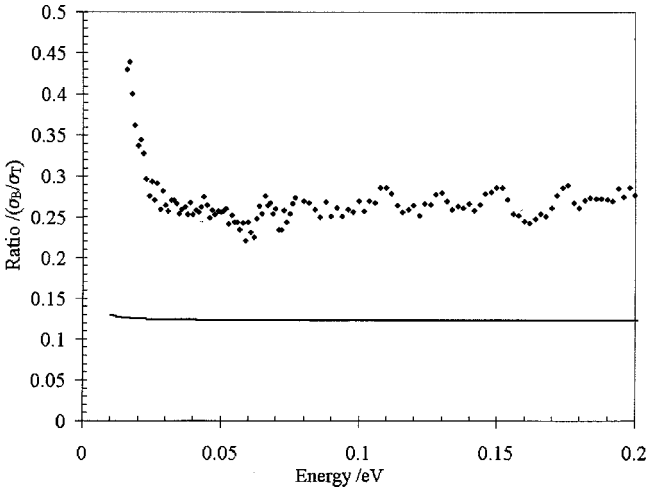

FIG. 6. CF_2Cl_2: ratios of backward to integral scattering cross sections (σ_B/σ_T) as a function of electron impact energy between 10 and 200 meV. Points: experimental values. Solid line: calculated using the first order Born point-dipole approximation.

Data in recent swarm studies in Ref. 9, which also reviews earlier data, show that CF_2Cl_2 attaches electrons at energies down to 40 meV, with rate coefficients showing a weak increase with decreasing electron energy below 200 meV. These data imply that the cross section increases with decreasing electron energy with a dependence lying between $E^{-1/2}$ and E^{-1}, consistent with *s*-wave attachment.[57,58] Dissociative attachment studies in Ref. 20 show a cross section increasing strongly with decreasing electron impact energy down to energies of a few meV, with ~7 meV energy resolution. These data therefore also show that an s-wave process is dominant in low energy dissociative attachment to yield Cl^-. This is confirmed in the data of Refs. 16, 17, 21, 59. With respect to possible contributions from *p*-wave scattering, this is allowed both electronically and vibronically, via B_1 ($\nu_{6,7}$) and B_2 vibrations ($\nu_{8,9}$).[4] However, Fig. 6 shows that our present data display close to backward–forward symmetry at the lowest impact energies. These results imply only a few percent of *p*- or higher angular momentum wave involvement at 20 meV impact energy.[26] Since pure rotationally inelastic events show strong forward-scattering, the observed angular behavior demonstrates that processes, which we suggest below are related to attachment, dominate over the electron-dipole interaction at very low impact energies.

A number of investigations, e.g., Ref. 9, show that the attachment rate coefficient for CF_2Cl_2 is enhanced by raising the temperature of the target gas. This effect is most marked at the lowest electron impact energies, in accordance with data from beam studies for dissociative attachment for the production of Cl^- from CF_2Cl_2.[19,59] Results obtained with the Laval nozzle technique [''CRESU'' (Ref. 60)] show that this trend continues to lower temperatures with rate coefficients for attachment dropping sharply below 300 K as both electrons and the molecular target are cooled. Various authors have suggested (see Refs. 19 and 60) that this is indicative of the presence of a small activation energy barrier to dissociative attachment.

Cross sections for dissociative attachment in room temperature gas at a few tens of meV energy impact energy have been reported to be only a few $Å^2$.[9,17,21] The true cross sections for dissociative attachment at low energy are certainly larger, since higher values at low energies are masked by inadequate electron energy resolution in the available data. Notwithstanding, it is evident that dissociative attachment cannot account for total integral scattering cross sections exceeding 350 $Å^2$ at an electron impact energy of 20 meV (Fig. 3).

Short-lived attachment in the absence of dissociative attachment provides a mechanism to explain our observations. This involves $CF_2Cl_2^-$ formation but with lifetimes too short for efficient Cl^- production, consistent with inhibition through the presence of an activation energy barrier (see above). Scattering through short-lived attachment reflects the fact that there is a set of states of the system only partially relaxed in the nuclear coordinates in the three-dimensional representation [potential energy]–[electron–CF_2Cl_2 separation]–[relaxation coordinate (e.g., C–Cl bond)]. As discussed at length in Ref. 9, in the absence of relaxation of the nuclear framework, $CF_2Cl_2^-$ may be accessed 0.9 eV above the ground state of the neutral, measured by the vertical attachment energy associated with the low-lying shape resonance (see Fig. 2). If the target becomes fully relaxed, the state of the system lies 0.4 eV below that of the neutral, corresponding to the value of the electron affinity of CF_2Cl_2. These two limiting cases of $CF_2Cl_2^-$ formation both involve the electron entering an a_1 orbital. For resonant attachment to take place there must be one or more bound states in the electron–CF_2Cl_2 attractive well. The scattering mechanism suggested to explain the present data requires that paths followed by the system feel the presence of these scattering states, which with sufficient time evolve into bound states of $CF_2Cl_2^-$ in which the electron has entered an a_1 orbital. Thus a set of encounters takes place which leads to resonant attachment followed by autodetachment. In these encounters the temporary negative ions do not have sufficient time to relax and cross the neutral potential surface. If trajectories were to cross this surface, true bound states of the system would form, energetically unable to eject the electron and by converting electron kinetic energy into nuclear kinetic energy would yield the competing (and weaker) channel of dissociative attachment. Essentially CF_2Cl_2 briefly captures an electron and the temporary negative ion undergoes autoionization before sufficient time has elapsed for dissociative attachment to take place. This mechanism requires that the scattering length of the system be positive and CF_2Cl_2 should therefore not show a Ramsauer–Townsend minimum (see above). In fact it is not possible to reconcile the presence of a Ramsauer–Townsend minimum with the marked dissociative attachment at near zero energy observed in CF_2Cl_2.[61,62]

Our conclusion is that CF_2Cl_2 may display a very interesting intermediate ''zero energy resonance'' case which involves temporary s-wave attachment. In contrast to SF_6,[64] CCl_4 or $CFCl_3$, resonant scattering states are short-lived leading to strong scattering but weak dissociative attachment. Thus unlike SF_6, CF_2Cl_2 does not steal the s-wave to make negative ions but rather scatters the s-wave with high cross section.

B. CF_3Cl

In our discussion of CF_3Cl data, we concentrate wholly upon the very low energy region below a few hundred meV. Higher energy scattering has been discussed in detail in Ref. 3. Results in Ref. 3 show clear evidence of a Ramsauer–Townsend minimum. Therefore CF_3Cl should not, in contrast to CF_2Cl_2, be a candidate for resonant s-wave electron attachment at very low energies since there is no bound state in the electron–CF_3Cl potential. Electron beam studies of dissociative attachment have been reported in Refs. 7, 18, 21–23. The authors in Ref. 18 note that dissociative attachment to form Cl^- is endothermic by ~0.1 eV and experiments in Ref. 18, albeit with an electron energy resolution of 0.1–0.2 eV, show that that Cl^- production is strongly enhanced for very low energy collisions when the target gas is heated and excited state populations of ν_3 are formed. Swarm studies[24,64] probe energies down to 0.4 eV and these again show that the temperature of the gas has a strong influence on electron attachment.

The mechanism of dissociative attachment is described in detail in Ref. 18, showing how excited vibrational wave functions may connect the neutral curve to the anion curve. Above the energy threshold, lying between $\nu_3=1$ and 2, this yields Cl^- products. We use related concepts in our attempt to understand our present scattering data for CF_3Cl. Note that dissociative attachment in CF_3Cl is a very weak channel, displaying cross sections of the order of only 0.15 $Å^2$ even in gas at 800 K.[13] Data in Ref. 21 cite a dissociative attachment cross section around zero energy of $\sim 2\times 10^{-3}$ $Å^2$ in room temperature gas, probably representative of the ~1% population of $\nu_3=2$ at 300 K.

Threshold vibrational excitation at 137.4 meV is observed in our data for the strong IR active CF_3 symmetric stretch (ν_1). The feature is experimentally quite weak, but clearly discernible in Fig. 4, with a cross section of ~1.5 $Å^2$ in integral scattering. The good precision of the onset energy, found experimentally at 136.5 meV, serves as a useful independent check of our electron energy calibration.

The major feature of the data in Fig. 4 is the suppression of rotational excitation between 40 meV and 100 meV. A few general points may be made about this relatively new phenomenon. (i) Suppression of rotational excitation is not a general phenomenon. We observe it in a disparate group of four molecules, CF_3Cl, ClO_2,[28] nitrobenzene,[26,27] and Cl_2O (unpublished work) but it is not found in numerous other dipolar species, such as CH_3OH, C_2H_5OH, NH_3, H_2S, C_6H_5X (X=F, Cl, Br, I) etc.[26] (ii) The effect is seen in forward scattering and is absent (or weaker) in the backward cross section. Hence numerous partial waves must be involved, each individually contributing only weakly to the phenomenon, as in rotationally inelastic scattering. (iii) The phenomenon shows that rotationally inelastic scattering cannot be treated independently of other scattering channels, since suppression must arise through a destructive interference involving two or more competing channels of scattering acting in superposition.

We first consider the behavior of the Born rotationally inelastic scattering cross sections in comparison with our data. Calculations were performed as described for CF_2Cl_2 and in detail in Ref. 5, using rotational constants for CF_3Cl taken from Refs. 65 and 66. Results are shown in Fig. 7. Backward scattering cross sections are too low, by a factor of 3–5, rather less than the discrepancy encountered in CF_2Cl_2. Since Born theory predicts a monotonic increase in cross section with decreasing energy, theory clearly cannot reproduce the strong dip in the integral cross section below 100 meV. The Born result is markedly too low at energies above this dip, overestimates the cross section in the region of the experimental minimum and then records good agreement with measured values at energies below 50 meV.

We suggest the following qualitative explanation for our observations. As the electron impact energy increases from zero, the first vibrational effect will be that associated with the Raman active mode, ν_3, at 59 meV, of A_1 symmetry. By analogy with the description for the process of vibrational excitation in SF_6,[63] the excitation of this mode is associated with temporary negative ion formation. The symmetry of the LUMO is a_1,[3,6,10] and is therefore of the correct symmetry

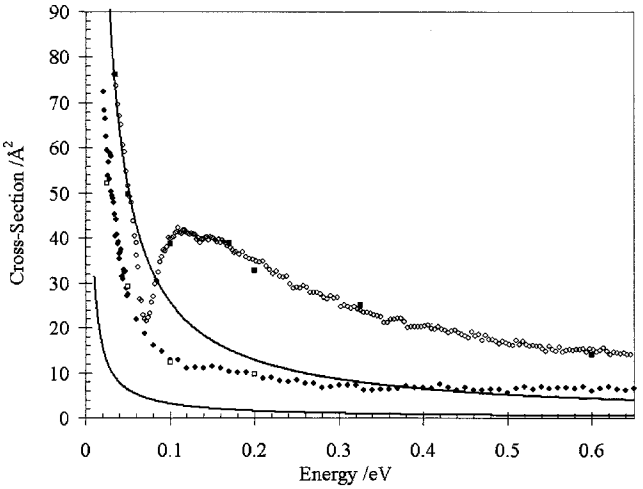

FIG. 7. CF_3Cl: experimental electron scattering cross sections vs electron energy as in Fig. 4 shown with cross sections calculated using the first order Born point-dipole approximation. Upper solid line: calculated integral cross sections. Lower solid line: backward scattering cross sections.

to excite the A_1 vibration. Moreover all partial waves, even and odd, have irreducible representations under the operations of C_{3v} which are A_1. Thus all partial waves, unlike the case of SF_6, may be involved in the essentially inseparable attachment and Raman vibrational excitation processes. Since the target has a dipole moment, high partial waves will be involved. These waves should contribute to a process which is overall strongly forward scattered, each component wave undergoing only a small phase shift. The temporary negative ion formed via vibrational excitation will in general autoionize to generate an overall process of rotationally and rovibrationally inelastic scattering.

Accompanying the indirect anion-mediated process of inelastic scattering is the direct Born-type process of rotationally inelastic scattering. By analogy with a Fano-type process,[67] the direct and indirect inelastic processes act in superposition, generating interference which appears in the inelastic scattering cross section. Interference in the present case is destructive at lower energies and constructive at higher energies. Given that the anion-mediated channel is only significantly active in the forward direction, interference is not apparent in the variation of the backward scattering cross section with energy. By analogy with SF_6, vibrational excitation persists strongly at energies extending beyond several hundred meV and anion-mediated enhancement of inelastic scattering may therefore explain the high integral cross sections in the hundreds of meV energy range in Fig. 4.

IV. CONCLUDING COMMENTS

Total integral and backward scattering cross sections for CF_2Cl_2 and CF_3Cl in the tens to hundreds of meV energy range show remarkably anomalous behavior. CF_2Cl_2 shows scattering cross sections considerably in excess of those expected for a molecule with a dipole moment of 0.5 D, and much greater than those observed for CF_3Cl, which has the same dipole moment. We attribute the behavior of CF_2Cl_2 to an additional channel involving short-lived negative ion for-

mation, the other side of the coin to the relatively weak channel involving dissociative attachment. CF_3Cl shows quite different behavior. In this case, rotationally inelastic scattering is suppressed over the range of energy between 50 and 100 meV. We attribute this to an interference between short-lived attachment, associated with the ν_3 Raman active vibration in CF_3Cl, and direct rotational scattering.

These data reinforce the view—based on similar data for more than 50 different species of very varied chemical nature—that we may lack even a qualitative grasp of the some important phenomena that occur when cold electrons encounter molecules. This is despite the interest in these processes, not only in industrial plasmas as outlined in the Introduction, but also in aeronomy and in cooling of electrons in the interstellar medium. The mechanisms which we propose in the present cases are plausible, but lack the sound support that theory should be able to provide.

ACKNOWLEDGMENTS

The authors would like to thank the Directors and Staff at the Institute for Storage Ring Facilities at Aarhus (ISA) and the Synchrotron Radiation Source (SRS) at Daresbury Laboratory for providing the facilities necessary for this work. J.P.Z. gratefully acknowledges financial support from the Royal Society (UK) under the European Science Exchange program, the CNRS (France)-Royal Society agreement and the CNRS-SNF (Denmark) agreement. We also thank the EPSRC for a PDRA position for R.J.G.

[1] A. Mann and F. Linder, J. Phys. B **25**, 533 (1992).
[2] A. Mann and F. Linder, J. Phys. B **25**, 545 (1992).
[3] A. Mann and F. Linder, J. Phys. B **25**, 1621 (1992).
[4] A. Mann and F. Linder, J. Phys. B **25**, 1633 (1992).
[5] J. Randell, J.-P. Ziesel, S. L. Lunt, G. Mrotzek, and D. Field, J. Phys. B **26**, 3423 (1993).
[6] T. Underwood-Lemons, D. C. Winkler, J. A. Tossell, and J. H. Moore, J. Chem. Phys. **100**, 9117 (1994).
[7] T. Underwood-Lemons, T. J. Gergel, and J. H. Moore, J. Chem. Phys. **102**, 119 (1995).
[8] L. G. Christophorou, J. K. Olthoff, and Y. Wang, J. Phys. Chem. Ref. Data **26**, 1205 (1997).
[9] Y. Wang, L. G. Christophorou, and J. K. Verbrugge, J. Chem. Phys. **109**, 8304 (1998).
[10] T. Beyer, B. M. Nestmann, and S. D. Peyerimhoff, Chem. Phys. **255**, 1 (2000).
[11] R. Curik, F. A. Gianturco, and N. Sanna, J. Phys. B **33**, 615 (2000).
[12] L. Lehr and W. H. Miller, Chem. Phys. Lett. **250**, 515 (1996).
[13] L. Lehr, J. Manz, and W. H. Miller, Chem. Phys. **214**, 301 (1997).
[14] A. P. P. Natalense, M. H. F. Bettega, L. G. Ferreira, and M. A. P. Lima, Phys. Rev. A **59**, 879 (1999).
[15] R. S. Wilde, G. A. Gallup, and I. I. Fabrikant, J. Phys. B **32**, 663 (1999).
[16] G. Denifl, D. Muigg, I. Walker, P. Cicman, S. Matejcik, J. D. Skalny, A. Stamatovic, and T. D. Märk, Czech. J. Phys. **49**, 383 (1999).
[17] J. D. Skalny, S. Matejcik, T. Kikoviny, J. Venco, G. Senn, A. Stamatiovic, and T. D. Märk, Int. J. Mass. Spectrom. **205**, 77 (2001).
[18] I. Hahndorf, E. Illenberger, L. Lehr, and J. Manz, Chem. Phys. Lett. **231**, 460 (1994).
[19] I. Hahndorf and E. Illenberger, Int. J. Mass Spectrom. Ion Processes **167**, 87 (1997).
[20] A. Chutjian and S. H. Alajajian, J. Phys. B **20**, 839 (1987).
[21] K. Aflatooni and P. D. Burrow, Int. J. Mass. Spectrom. **205**, 149 (2001).
[22] E. Illenberger, H.-U. Scheunemann, and H. Baumgärtel, Chem. Phys. **37**, 21 (1979).
[23] T. Oster, A. Kühn, and E. Illenberger, Int. J. Mass Spectrom. Ion Processes **89**, 1 (1989).
[24] S. M. Spyrou and L. G. Christophorou, J. Chem. Phys. **82**, 2620 (1985).
[25] R. K. Jones, J. Chem. Phys. **84**, 813 (1986).
[26] D. Field, S. L. Lunt, and J.-P. Ziesel, Acc. Chem. Res. **34**, 291 (2001).
[27] S. L. Lunt, D. Field, N. C. Jones, J.-P. Ziesel, and R. J. Gulley, Int. J. Mass. Spectrom. **205**, 197 (2001).
[28] D. Field, N. C. Jones, J. M. Gingell, N. J. Mason, S. L. Lunt, and J.-P. Ziesel, J. Phys. B **33**, 1039 (2000).
[29] S. L. Lunt, D. Field, S. V. Hoffmann, R. J. Gulley, and J.-P. Ziesel, J. Phys. B **32**, 2707 (1999).
[30] R. J. Gulley, T. A. Field, W. A. Steer, N. J. Mason, S. L. Lunt, J.-P. Ziesel, and D. Field, J. Phys. B **31**, 5197 (1998).
[31] S. L. Lunt, J. Randell, J.-P. Ziesel, G. Mrotzek, and D. Field, J. Phys. B **31**, 4225 (1998).
[32] J. R. Randell, S. L. Lunt, G. Mrotzek, J.-P. Ziesel, and D. Field, J. Phys. B **29**, 2049 (1996).
[33] Y. P. Song, D. Field, and D. F. Klemperer, J. Phys. D **23**, 673 (1990).
[34] P. W. May, D. F. Klemperer, and D. Field, J. Appl. Phys. **73**, 1634 (1993).
[35] R. J. Gulley, S. L. Lunt, J.-P. Ziesel, and D. Field, J. Phys. B **31**, 2735 (1998).
[36] R. J. Gulley, T. A. Field, W. A. Steer, N. J. Mason, S. L. Lunt, J.-P. Ziesel, and D. Field, J. Phys. B **31**, 2971 (1998).
[37] D. Field, D. W. Knight, G. Mrotzek, J. R. Randell, S. L. Lunt, J. B. Ozenne, and J.-P. Ziesel, Meas. Sci. Technol. **2**, 757 (1991).
[38] K. Radler and J. Berkowitz, J. Chem. Phys. **70**, 221 (1979).
[39] G. Martinez, M. Sancho, and F. H. Read, J. Phys. E **6**, 631 (1983).
[40] W. Sohn, K.-H. Kochem, K. Jung, and H. Ehrhardt, J. Phys. B **19**, 4017 (1986).
[41] W. G. Sun, M. A. Morrison, W. A. Isaaca, W. K. Trail, D. T. Alle, R. J. Gulley, M. J. Brennan, and S. J. Buckman, Phys. Rev. A **52**, 1229 (1995).
[42] K. Floeder, D. Fromme, W. Raith, A. Schwab, and G. Sinapius, J. Phys. B **18**, 3347 (1985).
[43] K. Rohr, J. Phys. B **10**, 2215 (1977).
[44] R. E. Kennerly, Phys. Rev. A **21**, 1876 (1980).
[45] J. Randell, S. L. Lunt, G. Mrotzek, J.-P. Ziesel, and D. Field, J. Phys. B **27**, 2369 (1994).
[46] D. Klar, K. Harth, J. Ganz, T. Kraft, M.-W. Ruf, H. Hotop, V. Tsemekhman, K. Tsemekhman, and M. Ya. Amusia, Z. Phys. D: At., Mol. Clusters **23**, 101 (1992).
[47] D. Field, G. Mrotzek, D. W. Knight, S. L. Lunt, and J.-P. Ziesel, J. Phys. B **21**, 171 (1988).
[48] C. E. Kuyatt, *Methods of Experimental Physics*, edited by B. Bederson and W. L. Fite (Academic, New York, 1968), Vol. 7A, Chap. 1, p. 43.
[49] R. K. Jones, J. Chem. Phys. **82**, 5424 (1985).
[50] P. D. Burrow, A. Modelli, N. S. Chiu, and K. D. Jordan, J. Chem. Phys. **77**, 2699 (1982).
[51] I. Shimamura, *Electronic and Atomic Collisions*, edited by D. C. Lorenta, W. E. Meyerhoff, and J. R. Peterson (Elsevier, Amsterdam, 1986), pp. 93–104.
[52] K. Takayanagi, *Electron–Molecule Collisions*, edited by I. Shimamura and K. Takayanagi (Plenum, New York, 1984).
[53] O. H. Crawford, J. Chem. Phys. **47**, 1100 (1967).
[54] H. Takeo and C. Matsumura, Bull. Chem. Soc. Jpn. **50**, 636 (1977).
[55] C. H. Townes and A. L. Schawlow, *Microwave Spectroscopy* (McGraw–Hill, New York, 1955).
[56] M. Mizushima, *Quantum Mechanics of Atomic Spectra and Atomic Structure* (Benjamin, New York, 1970).
[57] C. E. Klots, Chem. Phys. Lett. **38**, 61 (1976).
[58] F. B. Dunning, J. Phys. Chem. **91**, 2244 (1977).
[59] A. Kiendler, S. Matejcik, J. D. Skalny, and T. D. Märk, J. Phys. B **29**, 6217 (1996).
[60] J. L. Le Garrec, O. Sidko, J. L. Queffelec, S. Hamon, J. B. A. Mitchell, and B. R. Rowe, J. Chem. Phys. **107**, 54 (1997).
[61] T. F. O'Malley, Phys. Rev. **130**, 1020 (1963).
[62] J. R. Taylor, *Scattering Theory* (Wiley, New York, 1972).
[63] J. R. Randell, D. Field, S. L. Lunt, G. Mrotzek, and J.-P. Ziesel, J. Phys. B **25**, 2899 (1992).
[64] D. L. McCorkle, A. A. Christodoulides, L. G. Christophorou, and I. Szamrej, J. Chem. Phys. **72**, 4049 (1980).
[65] J. H. Carpenter, J. D. Huse, C. E. Small, and J. G. Smith, J. Mol. Spectrosc. **93**, 286 (1982).
[66] S. Giorgianni, R. Visinoni, A. Gambi, S. Ghersetti, F. Capellani, and G. Restelli, J. Mol. Spectrosc. **104**, 40 (1984).
[67] U. Fano, Phys. Rev. **124**, 1866 (1961).